Denaturation of a Protein Monitored by Diffusion Coefficients: Myoglobin

Jungkwon Choi and Masahide Terazima*

Department of Chemistry, Graduate School of Science, Kyoto University, Kyoto 606-8502, Japan

Received: February 22, 2002; In Final Form: April 29, 2002

Change of global protein structure as a function of concentration of a denaturant, guanidine hydrochloride (Gdn−HCl), was studied by using the laser-induced transient grating (TG) method for carboxymyoglobin (MbCO). From the time profile of the TG signal after the photodissociation reaction of the ligand, diffusion coefficients (D) of the protein were determined at various concentrations of the denaturant. The denaturation curve of MbCO monitored by D was compared with that monitored by the circular dichroism (CD) method. The $-m$ value and ΔG^0_{N-U} determined from the transition curve monitored by D are smaller than those obtained from the CD signal intensity. This noncoincidence of the two transition curves indicates that the global structure of Mb is still changing after the complete secondary structure (α-helices) deformation process. The smaller diffusion coefficient of unfolded MbCO compared to folded MbCO can be interpreted in terms of changes of the protein−water interaction and the surface roughness of the protein, which is due to the conformational change of the protein from the native to the unfolding state.

1. Introduction

Many soluble globular proteins can be reversibly unfolded by adding denaturant in the solution. Stability of the protein (free energy) can be determined by the analysis of the denaturant-induced unfolding curve as a function of the denaturant concentration.[1−3] The extent of the denaturation of the protein has been frequently monitored by, e.g., the circular dichroism (CD) method,[4,5] emission detection,[3] or absorbance change of chromophores.[5,6] Emission intensity or absorbance provides us information on rather local protein structural changes around the chromophores associated with the optical transition. The destruction (or formation) of the secondary structure (e.g., α-helices or β-sheets) can be monitored by the CD signal intensity. However, to understand the nature of protein stability of the structure, it would be essential to monitor the same denaturation process using other physical quantities. In particular, monitoring the global protein structure during the unfolding process should be very important to understand the (un)folding process. In this respect, the diffusion coefficient (D) is certainly a useful quantity to monitor the unfolding curve, because it is a fundamental physical parameter for the elucidation of a macromolecular size and shape. It also provides us information on surface corrugation and roughness of globular proteins. Despite these important issues, there has been almost no study of the denaturation experiment by monitoring D. In this paper, we report D of caroxymyoglobin (MbCO) as a function of concentrations of Gdn−HCl ([Gdn−HCl]), which is known to be a very effective denaturant.

For measuring D at various denaturant concentrations, we used the laser-induced transient grating (TG) technique. This TG technique can detect a spatial concentration modulation of chemical species induced by the laser irradiation.[7−14] From the temporal profile of the TG signal intensity, D of a molecule can be determined in a time domain within a very short time period (less than 100 ms). There are several advantages in the TG method for this study. First, since the measurement requires only hundreds of milliseconds order, we can neglect the influence of convection, which sometime disturbs the D measurement seriously. Second, we do not need any other data on the protein for the measurement of D, because D can be calculated directly from the decay rate of the signal. Therefore, the obtained value should be accurate without any ambiguity from other quantities. Third, the diffusion process is detected as molecular movement inside the solution. The interaction between the protein and a wall of a sample cell can be minimized.

Myoglobin is a typical globular protein. The protein structural deformation upon adding denaturants has been the subject of intense research.[2,15,16] It was found that myoglobin and apomyoglobin undergo a multistep deformation by the pH denaturation. The intermediate observed at around pH 4 is considerd to be a rather compact structure with a significant amount of the secondary structure (α-helices) but without the rigid tertiary structure and is referred to as a molten globule intermediate. However, in the urea or Gdn−HCl-denaturant experiment, the denaturation curve monitored by the CD intensity is well expressed by a two-state unfolding transition and any intermediate state has not been observed clearly. For studying the denaturation of Mb by the TG method, we used the photodissociation reaction of MbCO. By the photoexcitation of the heme, a diatomic molecule bound at the heme iron can be dissociated. In particular, carbon monoxide (CO) photodissociated from the heme escapes from the protein interior to the solvent almost completely (quantum yield = 0.96) and it takes several milliseconds to approximatly tens of milliseconds to come back to the protein depending on the concentration of CO in the matrix.[17−19] This is a suitable photoreaction to measure D by the TG method.

We successfully measure D of MbCO at various Gdn−HCl concentration and found that D of unfolded MbCO is about 4 times smaller than that of the native structure. The denaturation curve monitored by D was compared with that by the CD method. We found that these denaturation curves are different each other; in particular, the $-m$ value determined from the D measurement is much smaller than that from the CD measurement. The smaller diffusion coefficient of unfolded MbCO

10.1021/jp0256802 CCC: $22.00
Published on Web 05/25/2002

compared to folded MbCO can be interpreted in terms of changes of the surface roughness and of the protein by the denaturation.

2. Experimental Section

The experimental setup for the TG experiment was similar to those reported previously.[20,21] The second harmonic of Nd:YAG laser (Spectra-Physics Quantum-ray Model GCR-170-10, pulse width 10 ns) was used as an excitation beam and a He−Ne laser beam (594 nm) as a probe beam. The diffracted probe beam was isolated from the excitation laser beam with a glass filter (Toshiba R-60) and a pinhole, detected by a photomultiplier tube (Hamamatzu R-928), and fed into a digital oscilloscope (Tetronix TDS-520). The TG signal was averaged by a microcomputer to improve a signal-to-noise (S/N) ratio.

The repetition rate of the excitation laser was about 3 Hz. The size of the excitation beam at the sample position was ca. 1 mm o.d.. The irradiated volume is small (typically ca. 4×10^{-3} cm^3) compared with the entire volume of the sample solution. All measurements were carried out at room temperature.

The ellipticity of a protein at 223 nm was measured by a JASCO J-720 spectropolarimeter using a path length of 2 mm. All CD measurements carried out at room temperature.

For a transient absorption (TA) experiment, we used the same experimental setup as the TG measurement. The transmitted probe light intensity was detected by a photomultiplier and the time profile was recorded by the digital oscilloscope.

Horse-heart myoglobin (Mb) and guanidine hydrochloride (Gdn−HCl) were purchased from Nacalai Tesque Inc. MbCO was prepared according to the method as follows. Mb solution in 50 mM Tris−HCl buffer, pH 8, was put into a rubber-topped quartz cell and the concentration of MbCO was adjusted to be 150−200 μM. The deoxy form (DeoxyMb) was obtained by adding sodium dithionite to the Mb solution under a nitrogen atmosphere. Carbon monoxide was passed over the deoxy form sample for 30 min to yield the CO form (MbCO). The sample cell was again purged with N_2 gas for several minutes. Under this dilute-CO-concentration condition, the recombination between deoxyMb and the dissolved CO in the solution becomes slow enough to measure the diffusion coefficient. The sample solution was prepared just before the measurement. The TG experiment was carried out for about 2−3 h after the sample preparation. Absorption spectra taken before and after the TG experiments were indistinguishable, indicating that there was no significant sample decomposition.

The value of q was determined from the decay rate of the thermal grating signal of the reference sample, bromocresol purple, which gives rise to only the thermal grating signal due to the nonradiative transition within the pulse width of the excitation laser.

3. Analysis

The transient grating (TG) is created in the sample solution by crossing two coherent beams. The TG intensity under the experimental condition is proportional to the sum of squares of the refractive index (δn; phase grating) and the absorbance (δk; amplitude grating) changes, which are induced by the spatially modulated light intensity. The refractive index change mainly comes from the thermal energy releasing (thermal grating) and created (or depleted) chemical species by the photodissociation reaction of MbCO (species grating). On the other hand, the amplitude grating comes from the change of the absorbance at the pulse wavelength by photochemical reactions. Since the rate constant of the thermal grating signal should be $D_{th}q^2$ (D_{th} = thermal diffusivity of the solution, q = grating wavenumber), it is easy to distinguish the thermal grating component from the species grating signal. The TG signal can be expressed as follows.

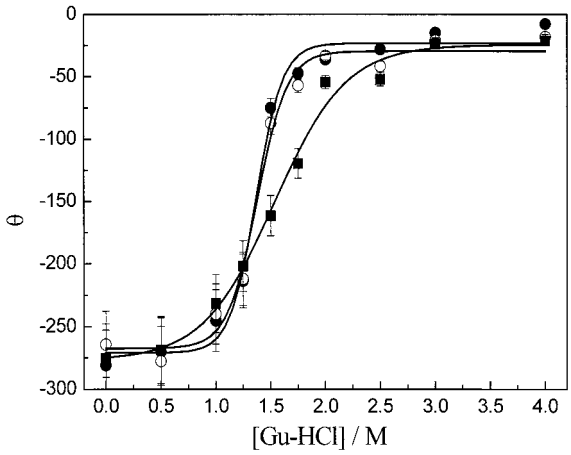

Figure 1. Gdn−HCl-induced denaturation curves of wild-type metMb (●), deoxyMb (○), and MbCO (■) monitored by the CD intensity at 223 nm in Tris−HCl buffer solutions (pH 8). Solid lines are the best fitted curve by eq 4.

$$I_{TG} = \alpha[\delta n]^2 + \beta[\delta k]^2 = \alpha[\delta n_{th} \exp(-D_{th}q^2t) + \sum_i \delta n_i \exp(-k_i t)]^2 + \beta[\sum_i \delta k_i \exp(-k_i t)]^2 \quad (1)$$

where α and β are a constant, δn_{th}, δn_i, and δk_i are the refractive index changes of the thermal grating, the species gratings, and the absorbance change of i species, respectively. k_i is the rate constant of each component.

The time evolution of the species grating signal intensity depends on the diffusion process of the species and concentration change due to a chemical reaction. When the reactant is regenerated from the product by a back-reaction with a rate constant k_{back}, the decay of the grating signal due to the i species is given by

$$k_i = D_i q^2 + k_{back} \quad (2)$$

where D_i is the diffusion constant of the chemical species. Therefore, the TG signal can be expressed as follows.

$$I_{TG} = \alpha[\delta n_{th} \exp(-D_{th}q^2t) + \sum_i \delta n_i \exp(-(D_i q^2 + k_{back})t)]^2 + \beta[\sum_i \delta k_i \exp(-(D_i q^2 + k_{back})t)]^2 \quad (3)$$

Thus, the diffusion constant of each component can be easily determined from the slope of the plot of the decay rate constant vs q^2.

4. Results

First, we examined the denaturation of wild-type metMb, deoxyMb, and MbCO using the CD detection. Figure 1 shows the Gdn−HCl-induced unfolding curve monitored by the CD

intensity at 223 nm in Tris−HCl buffer solutions (pH 8). This unfolding curve monitored by the CD intensity is well expressed by the two-state unfolding model as follows.

$$\theta_{223\mathrm{nm}} = \frac{\theta_{\mathrm{N}} - \theta_{\mathrm{U}}}{1 + \exp\{([\mathrm{G}] - [\mathrm{G}_0])/d\}} + \theta_{\mathrm{U}} \qquad (4)$$

where $\theta_{223\mathrm{nm}}$ is the ellipticity of each protein measured at 223 nm and θ_{N} and θ_{U} are the ellipticity of folded and unfolded protein, respectively. [G] is the concentration of a denaturant, d is a constant and $[\mathrm{G}_0]$ is the molar Gdn−HCl concentration at 50% denaturated. As shown in Figure 1, the unfolding midpoints are [Gdn−HCl] = 1.37, 1.38, and 1.52 M for metMb, deoxyMb, and MbCO, respectively.

For further investigation of the stability of Mb and the diffusion process, it is essentially important that the heme is intact in the protein part even under the denatured condition. Some papers suggested that the heme is detached from the protein when Mb is denatured.[22−25] However, contrary to these reports, we have confirmed that the heme is coordinated to the unfolded moiety by examining the reversibility of the denaturation as follows. If the heme is detached from the protein once, it will make an aggregation in the solution and it would not return back to the original position inside the protein even after refolding of the protein structure. We monitored the condition of the heme by measuring the absorption spectrum of the Soret band. This absorption spectrum is sensitive to the environment of the heme and reflects the binding condition. First we made metMb (150 μM) solution with [Gdn−HCl] = 3 M, under which condition metMb is unfolded, as shown in Figure 1. After several hours, the sample is diluted by the buffer solution so that [Gdn−HCl] becomes 0.3 M, under which condition metMb should have the native structure. We found that the absorption spectrum of the refolded sample is almost the same as the native metMb spectrum even 6 h after the denaturation. This reversibility ensures that the heme is not detached from the protein even under the denatured condition. This observation is consistent with results of earlier studies.[6,26] Moczygemba et al. reported that the unfolding of metMb was reversible (up to 5 M Gdn−HCl) and no protein concentration dependence was detected for the equilibrium unfolding transition, suggesting that the heme stays coordinated to the unfolded polypeptide.[26] Furthermore, by using the gel filtration method of unfolded holomyoglobin in up to 5 M Gdn−HCl, they also confirmed that the heme dissociation from His 93 did not occur in the range of [Gdn−HCl] ≤ 5 M. Hargrove et al. reported that the stability of Mb is enhanced ∼60-fold by reduction of iron to the ferrous deoxy state and ∼100-fold with CO coordination.[6] Indeed, by using the resonance Raman spectroscopic method, Sage et al.[27,28] and Han et al.[29] also reported that in MbCO, the majority of the heme-His 93 bond remains intact down to pH = 2.6. Therefore, we conclude that the heme stays inside the protein even under the unfolded condition we examine.

At each concentration of the denaturant, the free energy of unfolding, ΔG_{obsd}, was calculated using the following equation:

$$\Delta G_{\mathrm{obsd}} = -RT \ln[(x_{\mathrm{N}} - x_i)/(x_i - x_{\mathrm{U}})] \qquad (5)$$

where x_i is the numerical value of the structure-sensitive parameter at the ith denaturant concentration (i.e., the CD intensity in this case); x_{N} and x_{U} are the numerical values of the same parameter relative to the native and completely unfolded states, respectively. The free energy change for conversion of native to unfolding protein in the absence of denaturant ($\Delta G^0_{\mathrm{N-U}}$) and the $-m$ value was calculated from the plot of ΔG_{obsd} as a function of [Gdn−HCl] with an equation

$$\Delta G_{\mathrm{obsd}} = \Delta G^0_{\mathrm{N-U}} + m[\mathrm{Gdn-HCl}] \qquad (6)$$

$\Delta G^0_{\mathrm{N-U}}$ and $-m$ values of metMb, deoxyMb, and MbCO were determined from the plot of ΔG_{obsd} vs [Gdn−HCl] and these results are summarized in Table 1. $\Delta G^0_{\mathrm{N-U}}$ and $-m$ values of metMb are consistent with those of metMb reported by Moczygemba et al. ($\Delta G^0_{\mathrm{N-U}}$ = 5.45 kcal/mol and $-m$ = 3.37 kcal/(mol·M) at 20 °C).[26]

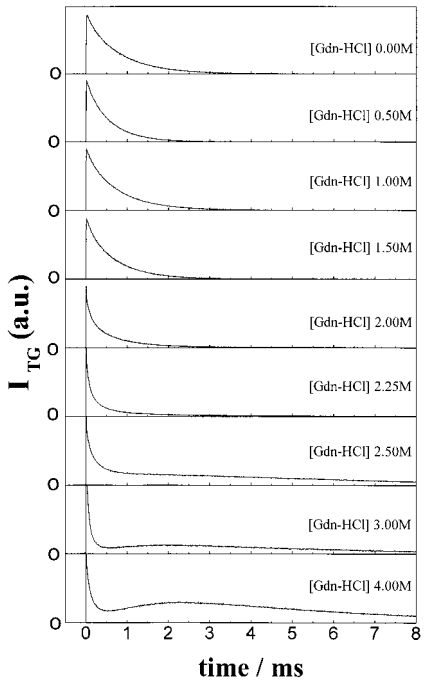

Figure 2. Species grating signals after the photodissociation of MbCO at various concentrations of Gdn−HCl.

TABLE 1: $\Delta G^0_{\mathrm{N-U}}$ and $-m$ Values of MetMb, DeoxyMb, and MbCO Determined from the Elliptisity at Room Temperature

	$\Delta G^0_{\mathrm{N-U}}$ (kcal/mol)	$-m$ value (kcal/mol, M)
MetMb	4.86 ± 0.5	3.47 ± 0.3
DeoxyMb	5.11 ± 0.5	3.74 ± 0.4
MbCO	3.00 ± 0.3	2.00 ± 0.2

Figure 2 shows the species grating signals after the photodissociation of MbCO as a function of [Gdn−HCl]. Since the decay of the thermal grating signal is very fast (∼1 μs), a contribution of the thermal grating signal in this time range can be neglected. In a range of 0−2 M Gdn−HCl concentration, the temporal profiles of the species grating signals are well reproduced by a single exponentional function. The decay rate gradually becomes faster with increasing [Gdn−HCl]. The species grating signal is dramatically changed with further increasing [Gdn−HCl]. In a range of [Gdn−HCl] ≥ 2.5 M, it shows a slower grow-decay feature beside the fast decay component (Figure 2).

For determining D from these signals, we have to consider the kinetics of chemical species in this photoreaction. Upon photoexcitation, MbCO is photodissociated to yield Mb and CO, and then Mb and CO recombine to recover MbCO. Thus three species, MbCO, Mb, and CO can contribute to the species grating signal. MbCO and Mb produce both the phase and amplitude gratings. On the other hand, CO only contributes to

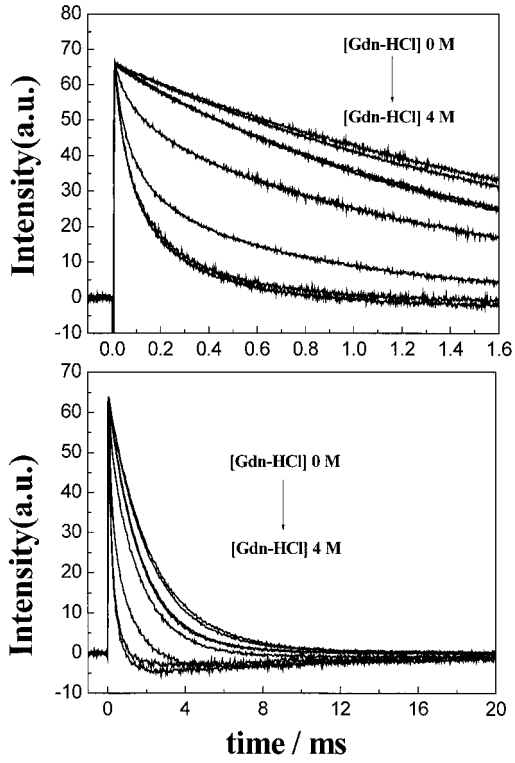

Figure 3. Absorbance change probed at 594 nm at various concentrations of Gdn−HCl (0, 0.5, 1.0, 2.0, 2.5, 3.0, and 4.0 M) after the photolysis of MbCO in pH 8 Tris−HCl buffer solutions.

the phase grating because there is no absorption band at the probe wavelength.

To investigate the kinetics of the reaction, we have measured the absorbance change probed at 594 nm as a function of [Gdn−HCl] following the photolysis of MbCO. The temporal profiles of the signals are shown in Figure 3. Under any Gdn−HCl concentration, the absorbance of the sample initially increased (enhanced absorption) after the photoexcitation. This enhanced absorption is consistent with the absorbance difference between deoxyMb and MbCO;[4,5] that is, the signal indicates the photodissociation of CO from the heme. The decay time at 0 M [Gdn−HCl] is well expressed by a single-exponential function and is attributed to the rate of the bimolecular recombination of CO and deoxyMb (DeoxyMb + CO → MbCO) under the present CO concentration. With the increasing denaturant concentration, the decay rate becomes faster. Interestingly, with further increase of [Gdn−HCl] (about 2.5 M), the signal initially shows enhanced absorption and then turns to a bleached signal. The temporal profile of the absorbance change under this condition must be fitted by a sum of three exponential functions; two exponentials for describing the decay of the enhanced absorption and one for the decay of the bleach signal. We found that the two decay rate constants of the enhanced absorption depend on the concentration of CO in the solution, whereas the slow rate constant for the bleach signal does not depend on [CO] (data is not shown). From this fact, we attribute the two fast decays of the enhanced absorption to the CO recombination process and the slow bleaching component is probably due to a conformational change of the protein. Although this is an intriguing observation to study the kinetics of the (un)folding process, the detail of the analysis is not a scope of the present study and the dynamics of the photodissociation of MbCO in the denatured state will be published elsewhere. An important point we should note in this study is

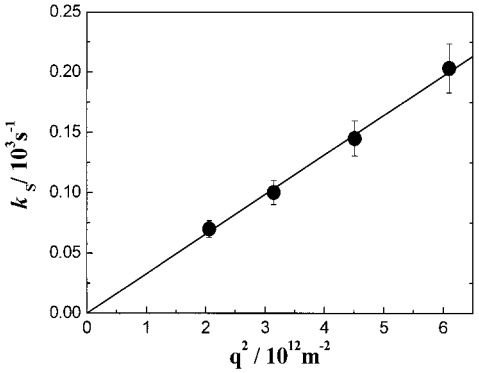

Figure 4. Plot of rate constants of the slow component against q^2 in 4 M Gdn−HCl solutions. Solid line is the least-squares fitted curve by $k = Dq^2$.

the presence of the transient species on tens of milliseconds time scale, which is necessary for the TG measurement.

From the slopes of the plot of the decay rate constant vs q^2, the diffusion constant in 0 M Gdn−HCl solutions is determined to be $(1.29 \pm 0.13) \times 10^{-10}$ m^2/s. Since this diffusion constant is significantly smaller than that of CO (2.6×10^{-9} m^2/s)[11] reported previously but rather close to that of Mb ($1.12-1.20 \times 10^{-10}$ m^2/s),[11,30,31] we can easily identify the origin of the decay component to the diffusion of protein. Therefore, the decay of the species grating signal observed in 0−2 M Gdn−HCl solutions represents the diffusion process of MbCO and the recombination of deoxyMb and CO ($D_{Mb}q^2 + k_{back}$), as expressed in eq 2. However, the species grating signal due to CO is too weak to be detected. This selective detection of Mb is what we expected, because the 594 nm probe light in this study is on resonance to the optical transition of Mb.

On the other hand, the temporal profile of the species grating signals observed in ≥ 2.5 M Gdn−HCl solutions is well reproduced by a sum of three exponential functions expressed as

$$I_{TG} = \alpha[\delta n_f \exp(-k_f t) + \delta n_i \exp(-k_i t) + \delta n_S \exp(-k_S t)]^2 + \beta[\delta k_f \exp(-k_f t) + \delta k_i \exp(-k_i t) + \delta k_S \exp(-k_S t)]^2 \quad (7)$$

where k_f, k_i, and k_S are the rate constants of the fast, intermediate, and slow components, respectively. $\delta n_{f(i,S)}$ and $\delta k_{f(i,S)}$ are the refractive index changes and the absorption changes associated with the fast, intermediate, and slow processes. We found that k_f and k_i are close to the rate constants observed by the absorption change (two decay components of the enhanced absorption). Therefore, these kinetics represent the recombination process of Mb and CO. For the fitting of the TG signal, we fixed k_f and k_i to the corresponding rate constants determined by the absorption detection in order to reduce the number of the adjustable parameter. We found that the rate constant of the slow decay component (k_S) depends on q^2, indicating that the signal is governed by the diffusion process in the solution. As described in the analysis section, k_S should be equal to $Dq^2 + k$, where k is the decay rate of the bleach component of the transient absorption signal.

Figure 4 shows the plot of k_S against q^2 in 4 M Gdn−HCl solutions. This rate constant shows a good linear relationship against q^2, as expected. From the slope of the plot, the diffusion constant in 4 M Gdn−HCl solution is determined to be $(0.32 \pm 0.03) \times 10^{-10}$ m^2/s. This diffusion constant is remarkably smaller than that of folded MbCO measured in 0 M Gdn−HCl solutions [$(1.29 \pm 0.13) \times 10^{-10}$ m^2/s]. Considering the magnitude of D, we can assign the chemical species of the slow

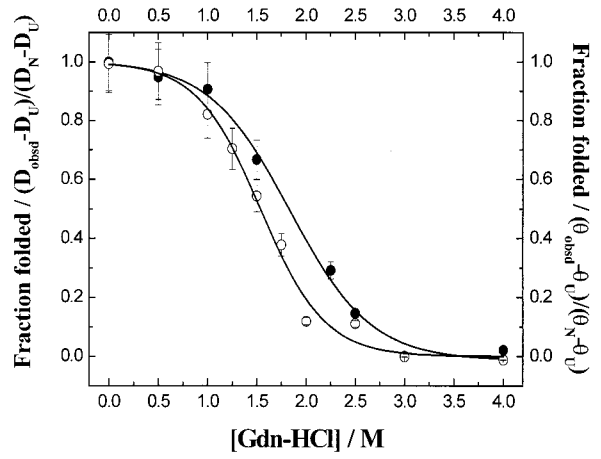

Figure 5. Changes of the diffusion constant (●) and the molar ellipticity (○) of Mb as a function of the concentration of Gdn−HCl. Solid lines are the best fitted curves by eq 4.

decay component to the unfolded MbCO. Figure 5 shows changes of the diffusion constant (D) and the ellipticity (θ) of Mb as a function of the concentration of Gdn−HCl.

5. Discussion

Here we consider the smaller diffusion coefficient of unfolded MbCO observed in this study. D does not reflect the real radius of the diffusing species but rather a hydrodynamic radius, which gives us an intuitive sense on the radius of a protein and its interaction. In this study, we found that D of the unfolded Mb is significantly smaller that that of the native Mb; the hydrodynamic radius of unfolded Mb (R_U) is 4 times larger than that of native Mb (R_N). The ratio of these values ($R_U/R_N \cong 4$) is large compared to the value of 2.3 for Mb obtained from the sedimentation experiment.[32] However, we should note that the diffusion constant of native Mb measured by the sedimentation experiment (0.99×10^{-10} m^2/s) is smaller than that reported recently [$(1.12-1.20) \times 10^{-10}$ m^2/s][11,30,31] and also determined in the present study [$(1.29 \pm 0.13) \times 10^{-10}$ m^2/s]. We think that this discrepancy comes from the uncertainty of the sedimentation experiment. Kawahara[32] and Williams et al.[33] reported a method to determine D of proteins from boundary spreading curves of a sedimentation experiment. They found that D determined by this method depends on the rotation speed, and the measurement should be carefully designed and corrected. The several uncertainties of the measurement may cause the smaller R_U/R_N from the sedimentation experiment compared with ours.

R_U and R_N are also reported for apoMb using the pH denaturation method and the light scattering technique.[34] The reported value of R_U/R_N ($\sim$2.1) is smaller than R_U/R_N in the present study. We think that the difference may come from the different denaturation condition. It is well-known that the confomation of the acid-induced denatured Mb is far from a randomly coiled polypeptide but is partially folded,[2,35,36] while the strong denaturant such as Gdn−HCl and urea can induce the complete denaturation of a protein.[35] Therefore, D_U obtained in this report represents D of a completely denaturated protein.

There are several factors that govern the diffusion process of molecules in solution, such as size, shape of the molecule, and the intermolecular interaction between the solvent and the diffusing molecules. To investigate the origin of the slow diffusion of the denatured MbCO, we first examine the effect of the molecular shape on D. According to the Stokes equation, the frictional coefficient (f_0) for a spherical molecule is expressed as follows.[37,38]

$$f_0 = 6\pi\eta R_0 \tag{8}$$

where η is the viscosity of the solvent and R_0 is the radius of a spherical molecule. When the shape is deformed from the spherical symmetry, the friction should be different from eq 8. A frictional ratio (f/f_0) for a prolate molecule was theoretically derived as[38]

$$f/f_0 = \frac{(a/b)^{2/3}(1 - b^2/a^2)^{1/2}}{\ln[1 + (1 - (b/a)^2)^{1/2}]/(b/a)} \tag{9}$$

where a is the semimajor axis and b is minor axis. If the molecule possesses a rodlike shape, f/f_0 is given by[38]

$$f/f_0 = \frac{(2/3)^{1/3}(a/b)^{2/3}}{\ln[2(a/b) - 0.30]} \tag{10}$$

For the native Mb, the ratio of the long to short axis is 1.105 and it can be treated as a spherical shape.[39] However, when the protein is denatured, the shape should be deformed from the spherical shape. Since we do not know the exact shape of the denatured Mb, let us consider D under an extreme condition. If the denatured Mb conformation is completely stretched, it could be considered as a rodlike shape. The a and b in this case are calculated to be roughly $a/b = 40$. Using eq 9 and 10, f/f_0 values of this protein are respectively calculated to be 2.7 and 2.3, which are smaller than that observed here. In a real condition, the shape of the denatured Mb cannot be a completely stretched form and f/f_0 could be much smaller. On the basis of these considerations, we think that the change of the shape of the protein is not the main origin of the smaller D under the denatured condition.

On the other hand, the interaction between a protein and water molecules will affect the frictional ratio, and indeed, some examples were reported by Tanford et al.[40] In the high-concentration of Gdn−HCl, the protein is completely denaturated and consequently the solvent-exposed surface area of the protein increases, indicating the increase in the binding site of Gdn−HCl and water upon a protein. Hence the solvent molecules will interact with a more corrugated protein surface and consequently the protein molecule feels more frictional drag in the solvents and its dynamic flexibility is more restrained. Choi et al. reported that the correlation dimension (D_2) value, which is a parameter describing the surface roughness of a protein molecule, is related to the diffusion coefficient.[41] The lager D_2 is, the smaller the diffusion coefficient is. From a point of view of this treatment, the large value of R_U/R_N (or the smaller D of unfolded MbCO) observed in this study is probably due to the significant increase of the surface roughness of a protein following the denaturation of a protein.

As shown in Figure 5, changes of D with the increasing concentration of Gdn−HCl are similar to those measured from the CD signal intensity, but slightly different each other. The midpoint of the transition curve monitored by D is shifted to 1.8 M from 1.52 M obtained by the CD measurement, and the transition region of the transition curve is wider than that obtained from the CD intensity

The denaturation monitored by D starts around [Gdn−HCl] $\approx$ 1.0 M, which is similar to the starting point for the denaturation monitored by the ellipticity. This fact may indicate a collective destruction of the secondary and the ternary structure. Another possible reason for this coincidence is that

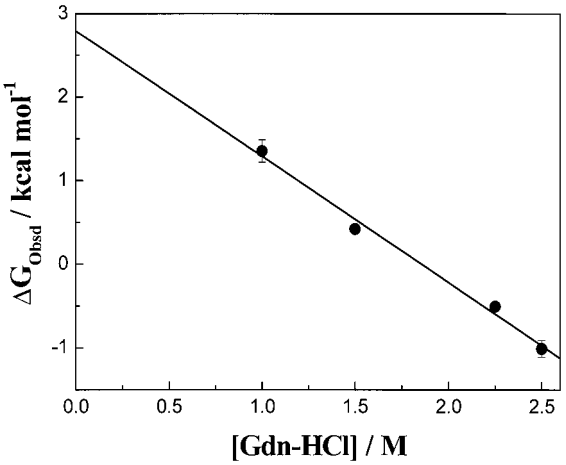

Figure 6. Change of the Free energy (ΔG_{obsd}) calculated from the diffusion constant of Mb as a function of the concentration of Gdn−HCl. The solid line is the best fitted curve by eq 6.

the diffusion becomes slower due to the hydrophilic interaction between the water and the hydrophilic part that was protected in the α-helices of the native state but exposed to water in the denatured state.

It is interesting to note that, even after the complete denaturation process of the secondary structure around [Gdn−HCl] ≈ 2.0 M, the *D* value still changes by increasing [Gdn−HCl]. This delay indicates that the global structure of Mb is still changing even after the secondary structure, α-helices, is destroyed. Bismuto et al. measured denaturation curves monitored by the CD intensity and the absorption of the Soret band and found that the both curves are very similar.[42] The result indicates that the local structure around the heme is controlled by the destruction of the secondary structure and it is complete at [Gdn−HCl] > 2.0 M. Irace et al. studied the effect of Gdn−HCl on the denaturation around the heme site, the N- and C-terminal domains.[35] The denaturation processes were quite different from each other but the denaturation of every site is complete at [Gdn−HCl] ≈ 2.0 M. According to these data, the rather local structure around the heme and the secondary structure are completely destroyed at [Gdn−HCl] ≈ 2.0 M. However, our studies here indicate that the tertiary structure is not denatured completely even after the secondary structure vanishes. In the pH denaturation experiments, a compact globular state with a significant secondary structure (molten globule state) was observed.[2,36,43,44] In the GdnHCl=induced unfolding process, an intermediate state that has a structure similar to that of the pH-induced unfolding has been suggested.[35] However, the transient state observed here should be distinct from these states, because the secondary structure is completely lost in this new phase.

From the plot of ΔG_{obsd} vs [Gdn−HCl] shown in Figure 6, ΔG^0_{N-U} and $-m$ values determined from *D* are determined to be 2.79 ± 0.3 kcal/mol and 1.51 ± 0.15 kcal/(mol·M), respectively (Table 1). This $-m$ value from *D* is much smaller than that from the CD signal intensity. Generally, in the denaturation process, changes in $-m$ values are indicators of the change in solvent-exposed surface area upon unfolding a protein. Alternatively, the different $-m$ value by monitoring different properties could be interpreted in terms of a more than two-state model. As mentioned above, the global change occurs roughly by a biphase event. Initially, the global structure changes with the destruction of the secondary structure and then is further destroyed after the protein completely loses the secondary structure. This biphase process may explain the different $-m$ values observed by the *D* and CD measurements.

Besides considering this discrete step scheme, it is possible that the global structure change occurs continuously. Since the *D* measurement in this study is a time domain on a hundreds of millisecond order, we hardly think that the global structure between the native and the denatured forms is completely averaged in this time scale. Hence, we preferably think that the global structure is gradually changing depending on [Gdn−HCl], not on the equilibrium between completely unfolded and native states; i.e., a continuous model could be appropriate to describe the denaturation curve of *D*. We should further investigate the denaturation process of the protein based on the continuum model using a time-resolved technique.

6. Conclusions

The diffusion coefficient of myoglobin as a function of the concentration of Gdn−HCl was measured for the first time by using a photodissociation reaction of MbCO and the laser-induced transient grating method. From the time profile of the TG signal, we found that the diffusion constant of the unfolded Mb is 4 times smaller than that of the native Mb. The $-m$ and ΔG^0_{N-U} values determined from the transition curve monitored by *D* are smaller than those obtained by the CD signal intensity. This difference indicates that the deformation of the tertiary structure occurs slowly relative to the unfolding of the secondary structure, α-helices. That is, the global structure of Mb is still changing after the secondary structure deformation process. The smaller diffusion coefficient of unfolded MbCO compared to folded MbCO is due to the change of the protein shape and the significant increase of the surface roughness of the protein following the conformational change from the native to the unfolding state.

Acknowledgment. A part of this study was supported by a Grant-In-Aid (No13853002) from the Ministry of Education, Science, Sports, and Culture in Japan, and Research Grants in the Natural Science from the Mitsbishi Foundation.

References and Notes

(1) Santoro, M. M.; Bolen, D. W. *Biochemistry* **1988**, *27*, 8063.
(2) Barrick, D.; Baldwin, R. L. *Biochemistry* **1993**, *32*, 3790.
(3) Sirangelo, I.; Bismuto, E.; Irace, G. *FEBS Lett.* **1994**, *338*, 1.
(4) Xie, X.; Simon, J. D. *Biochemistry* **1991**, *30*, 3682.
(5) Esquerra, R. M.; Goldbeck, R. A.; Kim-Shapiro, D. B.; Kliger, D. S. *Biochemistry* **1998**, *37*, 17527.
(6) Hargrove, M. S.; Olson, J. S. *Biochemistry* **1996**, *35*, 11310.
(7) Fayer, M. D. *Annu. Rev. Phys. Chem.* **1982**, *33*, 63.
(8) Eichler, H. J.; Gunter, P.; Pohl, D. W. *Laser Induced Dynamic Gratings*; Springer-Verlag: Berlin, 1986.
(9) Miller, R. J. D. In *Time-Resolved Spectroscopy*; Clark, R. J. H., Hester, R. E., Eds.; John-Wiley & Sons: New York, 1989.
(10) Takeshita, K.; Hirota, N.; Imamoto, Y.; Kataoka, M.; Tokunaga, F.; Terazima, M. *J. Am. Chem. Soc.* **2000**, *122*, 8524.
(11) Sakakura, M.; Yamaguchi, S.; Hirota, N.; Terazima, M. *J. Am. Chem. Soc.* **2001**, *123*, 4286.
(12) Dadusc, G.; Ogilvie, J. P.; Schulenberg, P.; Marvet, U.; Miller, R. J. D. *Proc. Natl. Acad. Sci. U.S.A.* **2001**, *98*, 6110.
(13) Terazima, M.; Tomioka, H.; Hirai, K.; Tanimoto, Y.; Fujiwara, Y.; Akimoto, Y. *J. Chem. Soc., Faraday Trans.* **1996**, *92*, 2361.
(14) Terazima, M. *Adv. Photochem.* **1998**, *24*, 255.
(15) Barrick, D.; Hughson, F. M.; Baldwin, R. L. *J. Mol. Biol.* **1994**, *237*, 588.
(16) Kay, M. S.; Baldwin, R. L. *Biochemistry* **1998**, *37*, 7859.
(17) Olson, J. S.; Phillips, G. N., Jr. *J. Biol. Chem.* **1996**, *271*, 17593.
(18) Jones, C. M.; Ansari, A.; Henry, E. R.; Christoph, G. W.; Hofrichter, J.; Eaton, W. A. *Biochemistry* **1992**, *31*, 6692.
(19) Springer, B. A.; Sligar, S. G.; Olson, J. S.; Phillips, G. N., Jr. *Chem. Rev.* **1994**, *94*, 699.
(20) Hara, T.; Hirota, N.; Terazima, M. *J. Phys. Chem.* **1996**, *100*, 10194.

(21) Terazima, M.; Hara, T.; Hirota, N. *Chem. Phys. Lett.* **1995**, *246*, 577.
(22) Hughson, F. M.; Baldwin, R. L. *Biochemistry* **1989**, *28*, 4415.
(23) Pinker, R. J.; Lin, L.; Rose, G. D.; Kallenbach, N. R. *Protein Sci.* **1993**, *2*, 1099.
(24) Lin, L.; Pinker, R. J.; Kallenbach, N. R. *Biochemistry* **1993**, *32*, 12638.
(25) Lin, L.; Pinker, R. J.; Phillips, G. N.; Kallenbach, N. R. *Protein Sci.* **1994**, *3*, 1430.
(26) Moczygemba, C.; Guidry, J.; Wittung-Stafshede, P. *FEBS Lett.* **2000**, *470*, 203.
(27) Sage, J. T.; Morikis, D.; Champion, P. M. *Biochemistry* **1991**, *30*, 1227.
(28) Sage, J. T.; Li, P.; Champion, P. M. *Biochemistry* **1991**, *30*, 1237.
(29) Han, A.; Rousseau, D. L.; Giacometti, G.; Brunori, M. *Proc. Natl. Acad. Sci. U.S.A.* **1990**, *87*, 205.
(30) Jürgens, K. D.; Peters, T.; Gros, G. *Proc. Natl. Acad. Sci. U.S.A.* **1994**, *91*, 3829.
(31) Papadopoulos, S.; Jürgens, K. D.; Gros, G. *Biophys. J.* **2000**, *79*, 2084.
(32) Kawahara, K. *Biochemistry* **1969**, *8*, 2551.
(33) Williams, J. W.; Baldwin, R. L.; Saunders: W. M.; Squire, P. G. *J. Am. Chem. Soc.* **1952**, *74*, 1542.
(34) Gast, K.; Damaschun, H.; Misselwitz, R.; Müller-Frohne, M.; Zirwer, D.; Damaschun, G. *Eur. Biophys. J.* **1994**, *23*, 297.
(35) Irace, G.; Bismuto, E.; Savy, F.; Colonna, G. *Arch. Biochem. Biophys.* **1986**, *244*, 459.
(36) Chi, Z.; Asher, S. A. *Biochemistry* **1999**, *38*, 8196.
(37) Edward, J. T. *J. Chem. Educ.* **1970**, *47*, 261.
(38) Van Holde, K. E.; Johnson, W. C.; Shing Ho, P. *Physical Biochemistry*; Prentice- Hall, Inc.: Englewood Cliffs, NJ, 1998.
(39) Smith, M. H. In *Handbook of Biochemistry and Molecular Biology*, 2nd ed.; Sober, H. A., Ed.; CRC Press: Boca Raton, FL, 1970; p C-10.
(40) Tanford, C. *Physical Chemistry of Macromolecules*; John Wiley & Sons: New York, 1961.
(41) Choi, J.; Kim, H.; Lee, S. *J. Chem. Phys.* **1998**, *109*, 7001.
(42) Bismuto, E.; Colonna, G.; Irace, G. *Biochemistry* **1983**, *22*, 4165.
(43) Goto, Y.; Fink, A. L. *J. Mol. Biol.* **1990**, *214*, 803.
(44) Hughson, F. M.; Wright, P. E.; Baldwin, R. L. *Science* **1990**, *249*, 1544.